Ground demonstration of planetary gas lidar based on optical parametric amplifier

Kenji Numata[1,a,b], Haris Riris[b], Steve Li[b], Stewart Wu[b], Stephan R. Kawa[b], Michael Krainak[b], James Abshire[b]
[a]Department of Astronomy, University of Maryland, College Park MD, USA 20742
[b]NASA Goddard Space Flight Center, Greenbelt MD, USA 20771

ABSTRACT

We report on the development effort of a nanosecond-pulsed optical parametric amplifier (OPA) for remote trace gas measurements for Mars and Earth. The OPA output has high spectral purity and is widely tunable both at near-infrared and mid-infrared wavelengths, with an optical-optical conversion efficiency of up to ~39%. Using this laser source, we demonstrated open-path measurements of CH_4 (3291 nm and 1651 nm), CO_2 (1573 nm), H_2O (1652 nm), and CO (4764 nm) on the ground. The simplicity, tunability, and power scalability of the OPA make it a strong candidate for general planetary lidar instruments, which will offer important information on the origins of the planet's geology, atmosphere, and potential for biology.

Keywords: Optical Parametric Amplifier, Lidar, DIAL, Space Instrumentation

1. INTRODUCTION

Laser remote sensing measurements of trace gases from orbit can provide unprecedented information about important planetary science and answers to critical questions regarding planetary atmospheres. Carbon dioxide (CO_2), methane (CH_4), and carbon monoxide (CO) are three very important greenhouse gases on Earth. Remote sensing of these gases will assist in understanding Earth's climate change and will help to reduce the uncertainty in the carbon budget. NASA's decadal survey [1] called for a mission to measure CO_2, CH_4, and CO. Remote measurements of CH_4, water (H_2O), and other biogenic molecules (such as ethane and formaldehyde) on Mars have important connections to questions related to the existence of life on Mars [2]. If localized, areas with higher gas concentrations will become a primary target of future landing missions. Our aim is to increase the accuracy of mapping these gases globally through Integrated Path Differential Absorption lidar (IPDA) measurements with much higher accuracies by developing a near-infrared (NIR) and mid-infrared (MIR) lidar transmitter. Most trace gases on Mars and Earth have suitable spectral absorption features in the NIR (1.5~1.6 μm) and the MIR (3~5 μm) regions. Our tunable laser transmitter and high sensitivity detectors at NIR and/or MIR when used in a sounding (surface reflection) mode enable IPDA measurements from orbit with modest laser power.

At the NASA Goddard Space Flight Center (GSFC), we are developing a laser transmitter system for both Mars and Earth applications. Our system is based on a nanosecond-pulsed optical parametric amplifier (OPA) pumped at 1064 nm with magnesium oxide-doped periodically-poled lithium niobate (MgO:PPLN) as the non-linear medium. The OPA is suited for this application since it has a sufficient wavelength tuning range for gas detections and it generates both NIR and MIR, whereas no traditional laser has the necessary high spectral purity, sufficient pulse energy, and wide tuning capability. The two outputs at NIR and MIR are called "signal" and "idler", respectively. The output wavelengths of signal and idler can be tuned by adjusting a seed laser in the OPA. While our primary target is CH_4 on Earth and Mars, the OPA approach will allow a new capability for general planetary lidar instruments. In parallel, we continue to examine narrower band sources such as Yb fiber amplifier pumped optical parametric oscillator (OPO) and stand-alone Er:YAG lasers. These may ultimately achieve higher wall-plug efficiency [3, 4]. However, the OPA clearly provides a convenient light source for the measurement of numerous gases.

[1] kenji.numata@nasa.gov; phone 1 301-286-0799

While many gas sensing lidar systems are based on OPO approaches [5~11], our OPA approach is simpler, especially when narrow-linewidth, high-power pump and seed lasers are available. Due to the optical feedback provided by the resonant cavity, an OPO generally offers higher output beam quality, narrower output linewidth, and higher electrical-to-optical efficiency. However, it is sensitive to alignment, does not allow easy continuous tuning, and requires more optics, electronics, and frequent adjustment. High nonlinearity of a quasi-phase matched device (such as PPLN) allows efficient generation of NIR and MIR energy even with the single-pass OPA configuration. We think the simplicity and robustness of the OPA's optical arrangement make it a strong candidate for space applications – particularly Earth remote sensing. This type of single-pass device previously required high pump peak power with picoseconds pulsewidths. However, nanosecond pulsewidths are required for gas sensing applications in order to obtain the narrower transform-limited linewidths needed to resolve target gas lines. This type of nanosecond OPA system based on PPLN was previously primarily constructed with Nd:YAG microchip pump lasers [12~15].

In this paper, we report on the setup of the developed OPA system and measurements of diurnal variation of Earth's atmospheric CH_4, CO_2, H_2O, and CO using horizontal absorption paths.

2. EXPERIMENTAL SETUP

2.1 Overview

We have built three OPA systems, designated as OPA system 1, OPA system 2, and OPA system 3 in this paper. Figure 1 shows the experimental diagram of OPA system 1. In this system, both signal (1573 nm) and idler (3291 nm) are used for the simultaneous measurements of CH_4 and CO_2 using the near and far targets (as shown in Fig. 2), respectively. A nonlinear crystal is pumped by a pulsed 1064 nm Nd:YAG laser and seeded by a continuous-wave distributed-feedback (DFB) laser diode (LD) through a Erbium doped fiber amplifier (EDFA). OPA system 2 has a similar setup, except that only the signal wavelength near 1651 nm is used for CH_4 and H_2O measurements using the far target. OPA system 3 is implemented upon OPA system 1 by swapping the non-linear crystal and the seed laser. Its idler at 4764.0 nm is used for the measurement of CO. No fiber amplifier is employed for the seed in OPA systems 2 and 3, since there was no fiber amplifier that works at their seed wavelengths. Table 1 summarizes the specifications for the three OPA lidar systems.

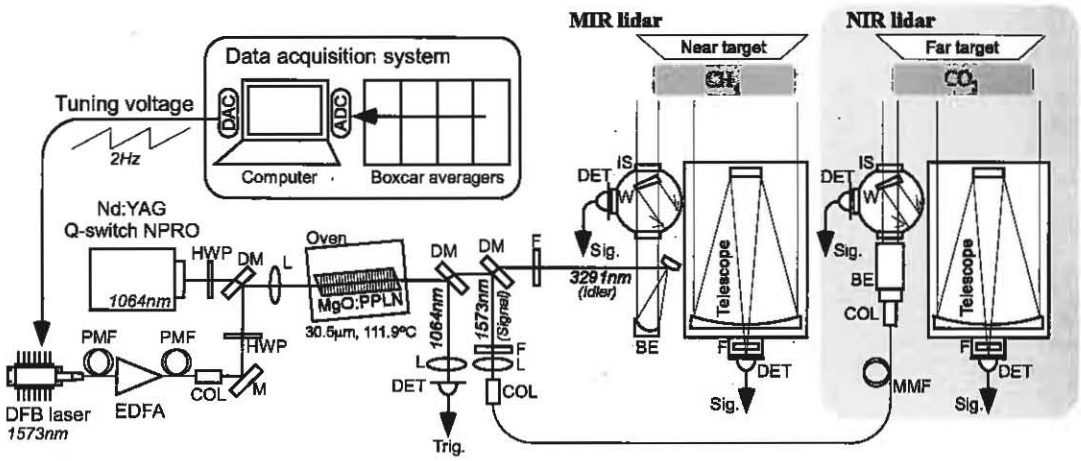

Figure 1. Experimental diagram. A MgO:PPLN crystal is pumped and seeded by a Q-switch Nd:YAG NPRO and a DFB laser, respectively. In OPA system 1 (1573 nm seed), both signal and idler are used for lidar measurement as shown in this figure. In OPA system 2 (1651 nm seed), only the signal is used for lidar measurement and there is no EDFA and MIR lidar. In OPA system 3 (1371 nm seed), only the idler is used for lidar measurement and there is no EDFA and NIR lidar. EDFA: Erbium-doped fiber amplifier, HWP: half wave-plate, M: mirror, DM: dichroic mirror, L: lens, F: wavelength-selecting filter, COL: fiber collimator, IS: integrating sphere, W: wedge, DET: detector, BE: beam expander, PMF: single-mode polarization maintaining fiber, MMF: multi-mode fiber, ADC: analog-to-digital converter, DAC: digital-to-analog converter, Trig.: trigger signal for boxcar averagers, Sig.: Signal input for boxcar averager.

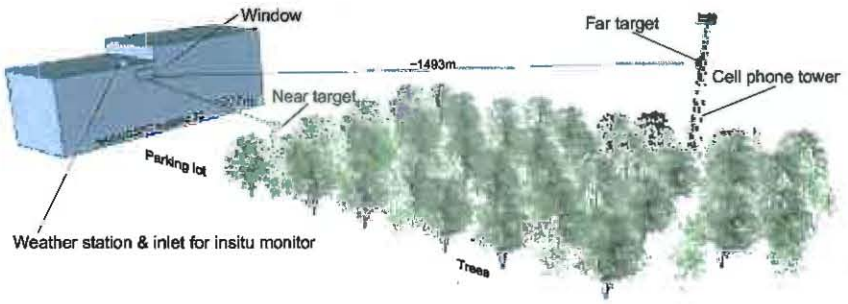

Figure 2. Schematic view of two open paths. The MIR lidars (idlers of OPA system 1 and 3) used the near target. The NIR lidars (signals of OPA system 1 and 2) used the far target.

	OPA system 1		OPA system 2		OPA system 3
Target gas	CH_4	CO_2	CH_4	H_2O	CO
(Wavelength)	(3291.1 nm)	(1573.3 nm)	(1650.9 nm)	(1652.0 nm)	(4764.0 nm)
Pumping					
Pump source	LD-pumped, passively Q-switched, Nd:YAG NPRO				
Pump pulse width	~3.3 nsec				
incident pump energy	~60 μJ				
Repetition rate	~6 kHz				
OPA					
Non-linear medium	MgO:PPLN, 50 mm(L) x 8 mm(W) x 1mm(H), 5° angle-cut, AR coated				
Grating period	30.5 μm		31.0 μm		26.4 μm
Temperature	111.9 °C		128.4 °C		109.5 °C
Beam radius	~100 μm for pump, ~125 μm for seed				
Output pulse width	~2 nsec				
Output energy	~7.6 μJ	~16 μJ	~13 μJ		~1.9 μJ
Output linewidth	~500 MHz				~700 MHz
Seeding					
Seed laser	Telecom DFB LD, PM fiber coupled				
Wavelength	1573.3 nm		1650.9nm/1652.0nm (temperature tuned)		1370.8 nm
Amplifier	PM EDFA		Not used		Not used
Seed power	~300 mW		~15 mW		~15 mW
Scan	2 Hz, ramped, current tuning				
Transmitter					
Integrated sphere coating	Infragold	Spectralon	Spectralon		Infragold
Beam expander	Reflective	Refractive	Refractive		Reflective
Wedge material	CaF_2	BK7	BK7		CaF_2
Receiver					
Telescope	200-mm diameter, Cassegrain				
Detector	HgCdTe	InGaAs	InGaAs		HgCdTe

Table 1. Technical data for the three OPA lidar systems.

2.2 OPA source

The pump source is a passively Q-switched Nd:YAG non-planar ring oscillator (NPRO) made by Innolight Inc. that emits single-frequency, single longitudinal-mode output at 1064.5 nm. It has ~3.3-nsec pulse width and ~60-μJ pulse energy at a ~6-kHz repetition rate. The optical linewidth of the NPRO is transform limited (~133 MHz).

The seed source is a continuous-wave, PM (polarization-maintaining) fiber-coupled, DFB LD. The instantaneous linewidth of DFB LD is less than 1 MHz. The wavelengths of the DFB LDs are selected to be 1573.3 nm, 1651 nm, and 1370.8 nm for OPA system 1, 2, and 3, respectively. The 1651-nm LD for OPA system 2 is step-scanned between 1650.9 nm and 1652.0 nm for CH_4 and H_2O measurements, respectively, by applying a step temperature change of 7.2 °C with an interval of 5 minutes. The DFB LD can be smoothly tuned through a wide range (>0.25 nm or ~30 GHz) without a mode hop, by injection current modulation. As a result, the output idler and signal can be tuned without a mode hop across the absorption peaks of the target gases. The seed LDs are tuned by a ramp voltage at 2 Hz. We observed that use of a higher seed optical power ensures smooth tuning as well as high efficiency. When the seed has low power and a slight misalignment, the signal was obscured by the amplified vacuum fluctuation and/or a parasitic parametric oscillation. Therefore, we used a minimum seed power of ~15 mW (for OPA system 2 and 3). For the OPA system 1 at 1573.3 nm, we amplified the seed to ~300 mW using a PM EDFA.

The seed beam is co-aligned with the pump using a dichroic mirror. The beams are focused down to a crystal by a lens with a focal length of 300 mm. The resultant beam radii inside the crystal are ~100 μm and ~125 μm for the pump and the seed, respectively. The locations of the beam waists are carefully adjusted to overlap with each other. With this pump beam size, the crystal is operated near the threshold of optical parametric generation (OPG).

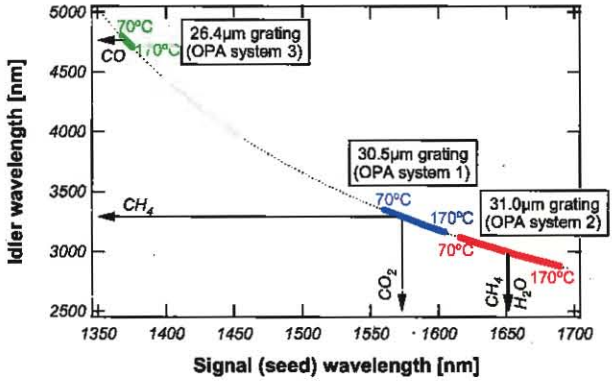

Figure 3. Tuning curves of the three MgO:PPLN crystals used in the three OPA systems. Wavelengths of the five gas absorption lines used in the lidar measurement are indicated by the arrows.

The nonlinear crystal is a 50-mm long, 1-mm thick MgO:PPLN. The end surfaces of the crystal were angled at 5° and anti-reflective (AR) coated at the pump, the signal, and the idler wavelengths in order to minimize optical feedback. A similar angle-cut crystal arrangement can be found, for example, in [16]. We observed that the output signal/idler wavelengths do not smoothly follow the scanned seed if the end surfaces of the crystal are not angled. Figure 3 shows the measured tuning curve of the MgO:PPLN crystals. We used a 30.5-μm grating at 111.9°C, 31.0-μm grating at 128.4°C, and 26.4-μm grating at 109.5°C for OPA systems 1, 2, and 3, respectively. The center wavelength of parametric gain at NIR was tuned around 1370 nm, 1575 nm, and 1650 nm, with the three gratings, by tuning the temperature between 70 and 170°C. The corresponding idler tuning occurred around 4770 nm, 3280 nm, and 3000 nm, respectively. The full-width half-maximum of the unseeded OPG spectra was about 0.3 nm, 1.2 nm, and 2.1 nm at 1370 nm, 1575 nm, and 1650 nm, respectively. As a result, the crystal temperature required no tuning for the two wavelengths (1650.9 nm and 1652.0 nm) in OPA system 2. Once seeded within the gain bandwidth, the output spectrum collapsed to the seed wavelength with >20dB suppression.

2.3 Lidar and monitor systems

The output beam is separated into three paths using dichroic mirrors. The signal at NIR and the idler at MIR are used for gas detection through open-paths with cooperative hard targets set at 1493 m and 207 m away, respectively, as shown in Fig. 2. The targets are covered by automotive reflective tape. The signal and the idler are detected by InGaAs and HgCdTe detectors, respectively. The light goes through a beam expander and a wedge, which is set inside the integrating sphere. The scattered light inside the integrating sphere is detected by a detector and used as an energy monitor to normalize the return signals. The return beams reflected by the hard targets are received by 20-cm Cassegrain telescopes with protective aluminum coatings. The pulsed signals from the detectors are averaged by boxcar averagers triggered by

the residual pump pulse. Optical crosstalk is avoided by inserting optical filters before the transmitter and after the telescope.

The temperature and pressure values of the atmosphere, which are needed to convert the measured absorption curve into mixing ratios, are monitored by a weather station set at the roof of our building. An in situ cavity ring-down spectrometer by Picarro Inc. monitors CH_4, CO_2, and H_2O mixing ratios of the outside air on the same roof. The lidar systems and the in situ system are set on the 4th floor of one of the buildings at GSFC, in Greenbelt, Maryland, United States.

3. EXPERIMENTAL RESULTS

3.1 OPA characterization

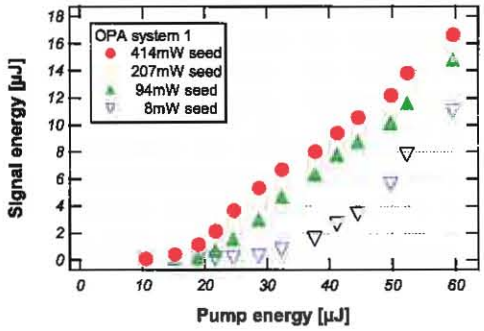

Figure 4. Relationship between signal and pump energies at different seed power levels (OPA system 1).

Figure 4 shows the relationship between pump energies, signal energies, and seed powers in OPA system 1. With a 60-μJ pump and a ~300-mW seed at 1573.3 nm, we obtained a ~16-μJ signal, excluding the effect of ~70-% transmittance of wavelength selection filter. The corresponding idler at 3291.1 nm was ~7.6 μJ. Thus, total pump conversion efficiency was (16 μJ+7.6 μJ)/60 μJ~39%.

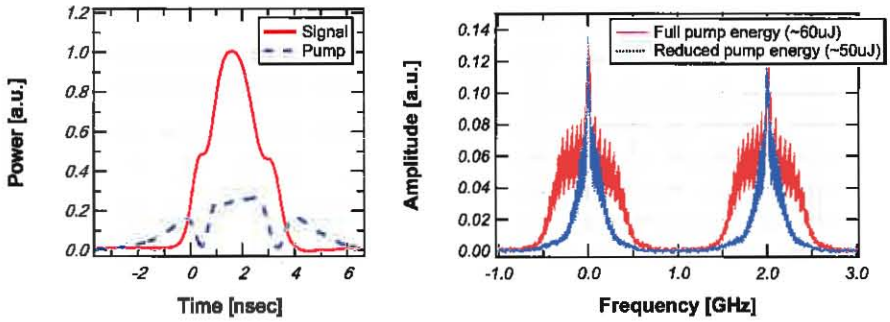

Figure 5. (Left) Typical pulse shapes of the output signal and residual pump. (Right) Typical optical spectrum of the output signal with full and reduced pump energies. This is measured by a scanning Fabry-Perot etalon with 2-GHz free spectral range.

As shown in Fig. 5 (left), the OPA output had a ~2-nsec width and a distorted Gaussian pulse shape, which is caused by the back-conversion process between the 1064-nm pump and signal/idler. The M^2 of the OPA output signal beam was ~1.3. The output linewidth of the OPA was estimated both from the scanning Fabry-Perot etalon and the gas cells. When the pump energy was low and the crystal was operated near the differential frequency generation (DFG) regime, the linewidth of the signal was measured as near transform limited (<200 MHz). When the pump energy was high and at our

nominal OPA operating condition, the signal was broadened to ~500 MHz (averaged over the beam) due to the back-conversion processes, as shown in Fig. 5 (right). The effect of the broadened linewidth on the measured mixing ratio was small, since the typical pressure-broadened full-width half maximum (FWHM) linewidth of our target line is ~5 GHz.

For the same seed power of ~15 mW, the total pump conversion efficiency was ~34%, ~33%, and ~14% for the OPA system 2 (1651-nm seed), 1 (1573-nm seed), and 3 (1371-nm seed), respectively. The higher efficiency for longer seed wavelengths can be partly attributed to the difference in the parametric gain, which becomes higher at longer seed wavelengths for the same crystal length and for the same optical power densities [17]. The low efficiency of the OPA system 3 (26.4-μm grating) was also thought to be a result of the imperfection of the crystal with a shorter grating period.

3.2 Open path scans

The calculation of the mixing ratio was done by fitting the scan result with theoretical Voigt profile (examples are shown in Fig. 6). To reduce the statistical error, 5 min of the digitized data were averaged. As a result, 10-min interval data of CH_4 and H_2O were alternatively obtained for OPA system 2. The signal from the receiver telescope was divided by the signal from the integrating sphere. The baseline was determined by fitting the divided data, excluding the absorption feature with a 5-th order polynomial function, which removed drifting instrumental fringes. The CH_4, CO_2, and CO absorptions are affected by the side lobes of nearby H_2O absorption lines and may cause error in the mixing ratio estimation. Therefore, the result from the 1652.0-nm H_2O lidar, which has less contamination from other gas species, was used to correct the baseline of the other lidar data. The data were normalized both by the fitted baseline and by the H_2O contribution, and finally fitted to the theoretical Voigt profile [18] using the center wavelength of the scan and a mixing ratio as the fitting parameters. The measured temperature, pressure, and round-trip path lengths were used to calculate the profile. Line parameters (center wavelength, line strength, etc.) are taken from the HITRAN 2008 database [19]. Ten adjacent lines were included into the fitting process.

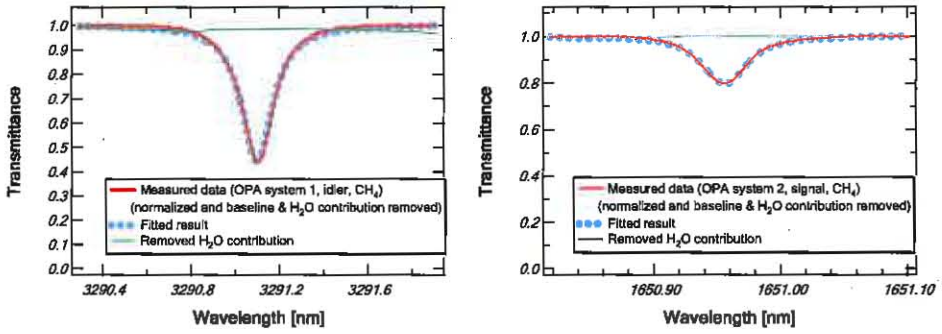

Figure 6. Examples of measured scan data and fitting results. CH_4 measurement at 3291.1 nm (left) and 1650.9 nm (right) are shown. The scan data were averaged, divided by the signal from the integrating sphere, and further normalized by a polynomial baseline determined from the edge of the data, after the removal of the H_2O contribution.

Figure 7 shows the result of simultaneous measurements of CH_4, CO_2, and H_2O mixing ratio over 50 hours (OPA system 1 and 2). The lidar measurements showed good agreement with in situ data for all three gases. Figure 8 shows the result of independent CO measurement (OPA system 3).

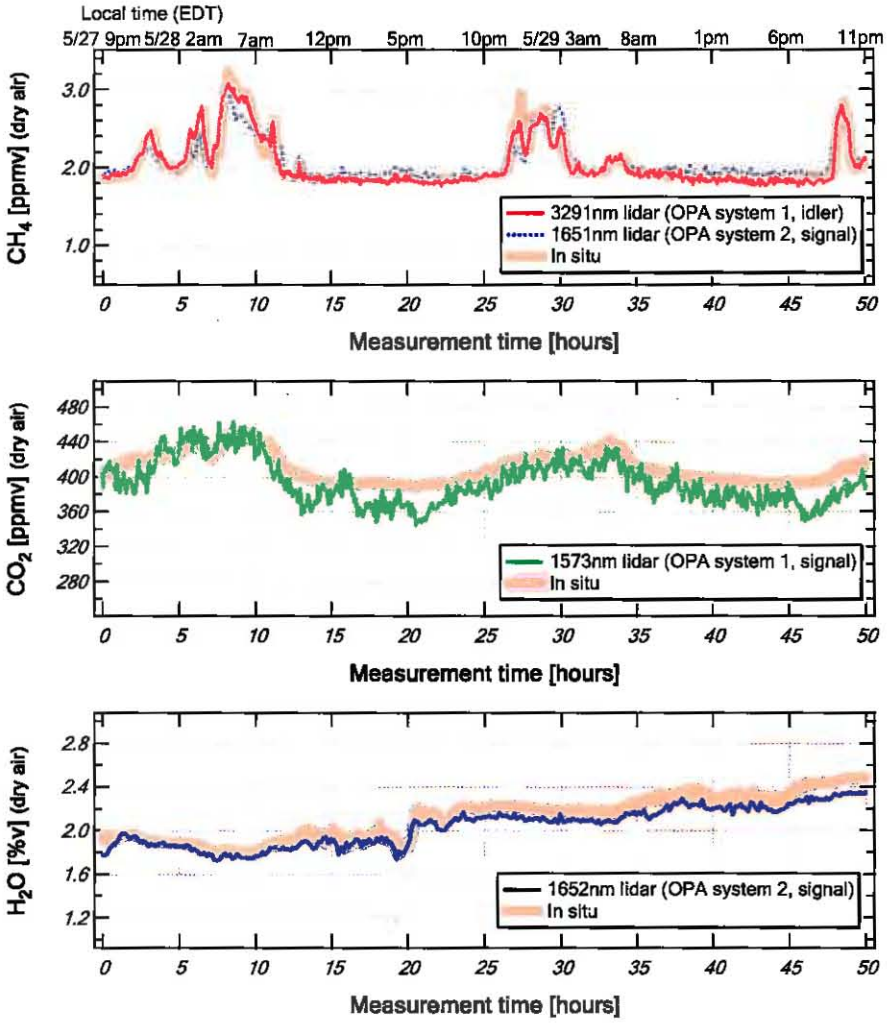

Figure 7. Simultaneous measurements of the diurnal variations of atmospheric CH_4 (top), CO_2 (middle), and H_2O (bottom) measured with OPA systems 1 and 2, and an in situ sensor.

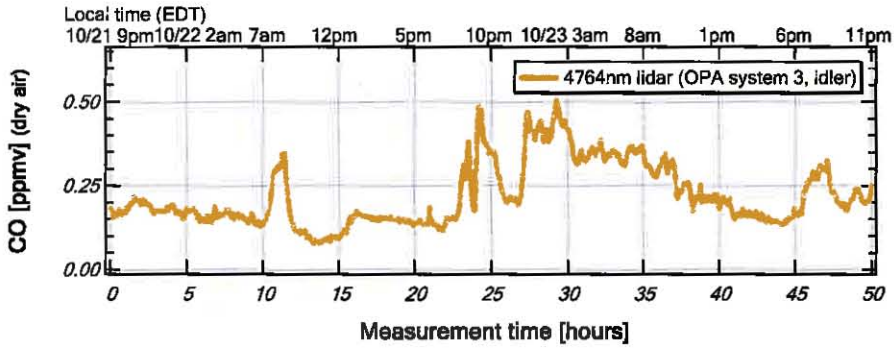

Figure 8. Measurement of the diurnal variation of atmospheric CO with OPA system 3.

4. DISCUSSION

4.1 Interpretation of results

The agreement between the lidar and the in situ sensor shows that the OPA system is capable of measuring variations in the mixing ratios of the atmospheric gases both at NIR and MIR. Their deviation can be largely explained by the difference between the lidar's column measurement and the in situ device's point measurement. We observed ~±0.5 ppm and ~±30 ppm mixing ratio variations in CH_4 and CO_2 channels, respectively. The source for the methane increase is thought to be the power plant at NASA GSFC, which uses natural gas from a nearby landfill. This hypothesis is in part supported by the difference observed between the two results from the two CH_4 channels. The 3291.1-nm channel (OPA system 1, near target) has a better agreement with the in situ data, while the 1650.9-nm channel (OPA system 2, far target) tended to show different CH_4 variations when increases occurred. This difference is possibly caused by the incoming CH_4 flow in the pipeline for the power plant. The CO_2 variation is equally likely to arise from respiration of vegetation at night. The larger fast fluctuation observed in the CO_2 channel is likely a result of the optical interference effects (etalon fringes) between the two ends of the multi-mode fiber. The H_2O channel (OPA system 2, far target) showed good agreement with in situ data, especially when no air-conditioning activity was ongoing in the building.

The CO diurnal variation measured by the 4764-nm channel (OPA system 3, near target) was the largest among the 4 measured species. This variation is most likely a result of car traffic activity. While this kind of dynamic CO variation was previously observed in early long-path measurements using a tunable diode laser [20], to the best of our knowledge, our measurement is the first CO open-path measurement based on OPA.

4.2 Airborne demonstration

We upgraded OPA system 2 and successfully performed an airborne measurement of CH_4 at 1650.9 nm from an 11-km altitude. A NIR photo-multiplier detected a strong return signal from the earth surface from a few km in altitude. The optics components were mounted on stable, spring-free mounts, and the fiber-coupled beam expander was replaced by a free-space transmitter. Instead of the continuous seed wavelength scan described in this paper, we implemented a stepped scan, which samples 20 wavelength points across the 1650.9-nm CH_4 line, pulse by pulse. These results will be reported in a separate paper. The successful flight demonstration confirmed that the OPA approach should enable IPDA measurements from orbit once the laser power is scaled up.

4.3 Power scaling for space implementation

Since our system is less sensitive to alignment, it can be implemented by naturally enhancing existing Nd:YAG space laser instruments. For satellite-based instruments at altitudes of a few 100s of km, our ~10-μJ output energy has to be scaled up by a factor of 20~50. In the experiment presented here, our output energy is limited by the pump energy (~60 μJ). Since this OPA approach should be scalable to a higher output power as long as the crystal is not damaged, we are looking into injection seeded NPROs and burst-mode Yb fiber amplifiers as ways to boost the pump energy to the >1mJ level. We have used a 600-μJ injection-seeded NPRO and have obtained a ~100-μJ signal output. The use of a fiber laser in burst mode is a new concept for OPA power scaling, and it potentially offers higher wall-plug efficiency for space applications. In these high pump energy situations, back-conversion would lead to spectral broadening and may obscure detailed spectral features of low-pressure atmospheres. For example, the Doppler width of a CH_4 line at 3270.4 nm is ~240 MHz for the Martian atmosphere (~5 Torr at the surface). Although the impact due to the broadened linewidth can be largely mitigated by data analysis, keeping the laser linewidth as narrow as possible is highly desirable. Therefore, we might need to make our OPA a multiple stage device and amplify a signal and/or an idler separately [21], especially for Mars applications, by using a longer pump pulse (~10 nsec) and larger beam size inside the crystal.

5. CONCLUSIONS

Lidar will be a key technology for the measurement of atmospheric gases with high sensitivity and resolution on global scales, and it will enhance our understanding of the current state of planetary atmospheres and geology. We have demonstrated the ability to detect diurnal variations of several atmospheric trace gases both in the NIR and MIR regimes, using OPA and cooperative hard targets. Comparative measurements of the CH_4, CO_2, and H_2O variations measured by the OPA systems and by an in situ instrument showed good agreement. We measured four important greenhouse gases

using the OPA for Earth applications. Given a sufficient tuning range of the OPA, the measurements can be extended to other molecules. We believe that our approach will become a core technology in future planetary lidar instruments.

This work is supported by the NASA Astrobiology Program's Astrobiology Science and Technology Instrument Development (ASTID) Program.

REFERENCES

[1] National Research Council, "Earth Science and Applications from Space: National Imperatives for the Next Decade and Be-yond," Jan. 2007, available from http://www.nap.edu/.

[2] G. L. Villanueva, M. J. Mumma, and R. E. Novak, "Strong release of methane on Mars: Evidence of biology or geology?," 19th Annual VM Goldschmidt Conference, Davos, Switzerland, *Geochimica et Cosmochimica Acta*, **73,** A1384 (2009).

[3] Y. Chen, F. Kimpel, J.-L. Fouron and S. Gupta, "MW+ peak power sub-nsec 10-kHz repetition rate polarization-maintaining fiber-amplifiers using tapered Yb-doped fibers," Proc. SPIE **8237,** 82371T (2012).

[4] D.-W. Chen, P. M. Belden, T. S. Rose, and S. M. Beck, "Narrowband Er:YAG nonplanar ring oscillator at 1645 nm," *Opt. Lett.* **36,** 1197 (2011).

[5] R. A. Baumgartner and R. L. Byer, "Continuously tunable ir lidar with applications to remote measurements of SO_2 and CH_4," *Appl. Opt.* **17,** 3555 (1978).

[6] M. J. T. Milton, T. D. Gardiner, F. Molero, and J. Galech, "Injection-seeded optical parametric oscillator for range-resolved DIAL measurements of atmospheric methane," *Opt. Comm.* **142,** 153 (1997).

[7] M. Imaki and T. Kobayashi, "Infrared frequency upconverter for high-sensitivity imaging of gas plumes," *Opt. Lett.* **32,** 1923 (2007).

[8] A. Amediek, A. Fix, M. Wirth, and G. Ehret, "Development of an OPO system at 1.57 μm for integrated path DIAL measurement of atmospheric carbon dioxide," *Appl. Phys. B* **92,** 295 (2008).

[9] D. Sakaizawa, C. Nagasawa, T. Nagai, M. Abo, Y. Shibata, M. Nakazato, and T. Sakai, "Development of a 1.6 μm differential absorption lidar with a quasi-phase-matching optical parametric oscillator and photon-counting detector for the vertical CO_2 profile," *Appl. Opt.* **48,** 748 (2009).

[10] A. Fix, C. Büdenbender, M. Wirth, M. Quatrevalet, A. Amediek, C. Kiemle, and G. Ehret, "Optical parametric oscillators and amplifiers for airborne and spaceborne active remote sensing of CO_2 and CH_4," *Proc. SPIE* **8182,** 818206 (2011).

[11] A. W. Yu, K. Numata, H. Riris, J. B. Abshire, G. Allan, X. Sun, and M. A. Krainak, "Mid-Infrared OPO for high resolution measurements of trace gases in the Mars atmosphere," in Laser Applications to Chemical, Security and Environmental Analysis, OSA Technical Digest (CD) (Optical Society of America), paper LMC5 (2008).

[12] J. Zayhowski, "Periodically poled lithium niobate optical parametric amplifiers pumped by high-power passively Q-switched microchip lasers," *Opt. Lett.* **22,** 169 (1997).

[13] K. Aniolek, R. Schmitt, T. Kulp, B. Richman, S. Bisson, and P. Powers, "Microlaser-pumped periodically poled lithium niobate optical parametric generator-optical parametric amplifier," *Opt. Lett.* **25,** 557 (2000).

[14] T. J. Kulp, S. E. Bisson, R. P. Bambha , T. A. Reichardt , U. B. Goers, K. W. Aniolek , D. A. V. Kliner, B. A. Richman, K. M. Armstrong, R. Sommers, R. Schmitt, P. E. Powers, O. Levi, T. J. Pinguet , M. M. Fejer, J. P. Koplow, L. Goldberg, T. G. Mcrae, "The application of quasi-phase-matched parametric light sources to practical infrared chemical sensing systems", *Appl. Phys. B* **75,** 317 (2002).

[15] T. A. Reichardt, R. P. Bambha, T. J. Kulp, and R. L. Schmitt, "Frequency-locked, injection-seeded, pulsed narrowband optical parametric generator," *Appl. Opt.* **42,** 3564 (2003).

[16] U. Bäder, T. Mattern, T. Bauer, J. Bartschke, M. Rahm, A. Borsutzky, and R. Wallenstein, "Pulsed nanosecond optical parametric generator based on periodically poled lithium niobate," *Opt. Comm.* **217,** 375 (2003).

[17] I. T. Sorokina and K. L. Vodopyanov (Eds), "*Solid-State Mid-Infrared Laser Sources*," Springer, (2003), ISBN 3540006214.

[18] E. E. Whiting, "An empirical approximation to the Voigt profile," *Journal of Quantitative Spectroscopy and Radiative Transfer*, **8,** 1379 (1968).

[19] L. S. Rothman, et. al., "The HITRAN 2008 molecular spectroscopic database," *Journal of Quantitative Spectroscopy and Radiative Transfer*, **110,** 533 (2009).

[20] R. T. Ku, E. D. Hinkley, and J. O. Sample, "Long-path monitoring of atmospheric carbon monoxide with a tunable diode laser system," *Appl. Opt.* **14,** 854 (1975).

[21] J. Burris and D. Richter, "Tunable infrared radiation for atmospheric profiling," *J. Appl. Remote Sens.* **2,** 023527 (2008).